Design of a Highly Efficient Microinverter

Omar Nezamuddin, Jonah Crespo, and Euzeli C. dos Santos Jr.

Indiana University-Purdue University Indianapolis,
Indianapolis, IN, 46202, USA

***Abstract* — This paper proposes a grid-tied single-phase photovoltaic (PV) microinverter consisting of five-level four-switch (5L-4S) DC-AC converter fed by an isolated fly-back DC-DC converter. The microinverter utilizes a split-coil inductor to produce five levels of pulse width modulation (PWM) compared to the three levels of PWM using conventional four-switch topologies. These implementations reduce losses by up to 39% compared to a conventional topology. The results show that the proposed design improves performance throughout the switching frequency spectra with various loads. The theoretical expectations are validated with simulation and experimental results.**

***Index Terms* — microinverter, energy conversion, photovoltaic system, power electronics.**

I. Introduction

In some solar systems, multiple solar panels are connected to a central inverter device which converts the direct current from the panels into alternating current. The panels are strung together in "Christmas light" fashion with the last and first panels connected to the central inverter [1]. While this approach has some benefits, the overall electrical output of the entire array may be greatly reduced by either partial obstruction of light to the array (e.g., shade, debris, snow, etc.), or malfunction of even a single panel. [2]. Consequently, many systems prefer the use of a microinverter mounted to each solar panel.

Microinverters are power electronic devices that convert DC power from a low power source, such as a solar panel, to AC power, such as that used in homes [3]. The main advantage of using a microinverter system to a string inverter system is that microinverters isolate light obstructions and faults from solar panels in the entire system [4]. A microinverter is constituted of two main conversion units: 1) a DC-DC boost converter to step up the DC voltage generated as well as guarantee its operation at maximum power, and 2) a DC-AC converter to generate a desired AC current to ensure a unity power factor with the connected grid.

Multi-level converters were first conceived for high voltage and high-power applications to implement DC-AC converters [5]. Since then, many configurations have been proposed [6,7] to establish the highly desirable characteristics for high-power applications, such as reduced waveform distortion and low blocking voltage by switching devices [8]. The three principal configurations are diode-clamped (or NPC), flying capacitor and cascade multi-level inverters [9,10].

More recently, multi-level converters have found acceptance in low power systems, especially in photovoltaic applications, since it is possible to generate high quality voltage waveforms with semiconductor switches operating at a frequency near the fundamental [11].

DC-AC multi-level converters for single-phase output has also been explored also explored in the technical literature due to its importance in low power applications [12-17]. For instance, [18] proposed a single-phase multilevel converter for application in electrified railway, while [19] proposed a family of single-phase multi-level inverters with the same number of switching devices as in the conventional topology but without clamping diodes and flying capacitors. More contributions for five-level output have been addressed in [20-23].

This paper proposed a microinverter based on a DC-AC converter with an optimized relationship between the number of output levels and number of power switches. Such a converter is able to generate an output voltage with five levels by using only four controlled power switches, which is by far the best relationship among the converters proposed in technical literature.

As shown in Fig. 1, a microinverter is characterized by its compact size. Notice from this figure that such a device is installed on the back of each panel. Therefore, size reduction is a priority when designing a microinverter. With the proposed microinverter topology, size of the device will be reduced via two methods. The first is by using a smaller filter to produce the same results as a conventional design in terms of output THD. Utilizing five levels of PWM voltage versus three gives the opportunity to reduce the output filter.

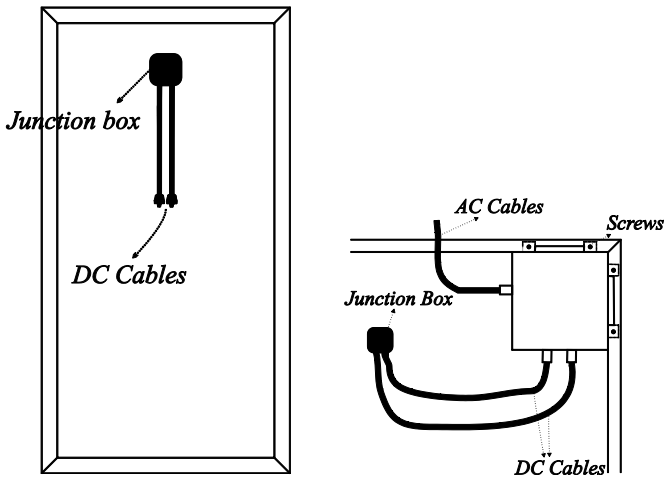

Fig. 1. (left) Back view of a solar panel, and (right) a microinverter installed on a solar panel.

This is the author's manuscript of the article published in final edited form as:
Nezamuddin, O., Crespo, J., & dos Santos, E. C. (2016, June). Design of a highly efficient microinverter. In Photovoltaic Specialists Conference (PVSC), 2016 IEEE 43rd (pp. 3463-3468). IEEE. https://doi.org/10.1109/PVSC.2016.7750310

The second is by using fewer components than conventional five-level inverters. Both neutral-point-clamp and flying capacitor topologies use more components than a four-switch five level (4S-5L) converter topology. Conventional designs would either add more switches or more capacitance than the proposed device, increasing the footprint of the entire system. The schematic highlighting the power components of the proposed microinverter is presented in Fig. 2.

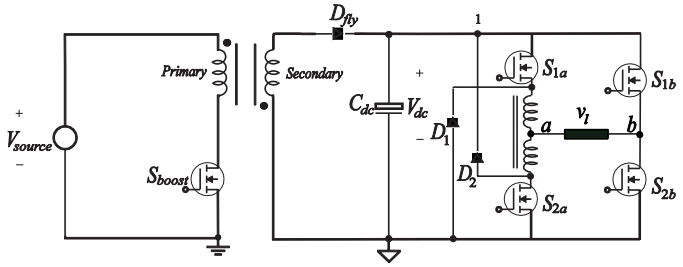

Fig. 2. Proposed microinverter schematic highlighting the power components.

II. Electrical Design Considerations

A. Block Diagram Representation

A block diagram representation with the main components is presented in Fig. 3. While dashed lines connected between these blocks represent signals, solid lines mean the power flow from different elements such as PV panel and utility grid. Notice from Fig. 2 that a fly-back DC-DC converter has been used in this design to isolate the DC and AC variables. For example, the power MOSFET S_{boost} is connected to the DC part of the circuit whereas the power MOSFETs S_{1a}, S_{2a}, S_{1b}, and S_{2b} are connected to the AC part of the circuit.

Therefore, all the circuitry necessary to generate the gating signals for each power switch must be also isolated and with different grounds.

B. Ground Isolation

An important aspect in a microinverter is having the voltage from the solar panel with a different reference than that of the grid [5]. As seen in Fig 3, the design of proposed microinverter includes two isolated grounds. The first is for the solar panel side, which will include the driver for the power switch implemented in the DC-DC converter. Notice that the voltage V_{cc1} employed to supply power to Driver 1 is obtained from the solar panel voltage. Therefore, the Voltage Regulator 1, Driver 1 and MOSFET S_{boost} shared the same ground.

The second ground will include the drivers for the power switches from the DC-AC converter (Driver 2 in Fig. 3), the microcontroller, Voltage Regulator 2, and current sensors. An important aspect of this design is that the microcontroller should be supplied by the utility grid since the control actions of the microinverter must be active with and without solar energy. On the other hand, in a black out situation the entire circuit should be disconnected from the grid, which could be obtained with a relay not presented in this figure.

C. Control Actions and Measurements

Sensor 1 will measure the PV panel voltage and current to implement the Maximum Power Point Tracker (MPPT) algorithm. Sensor 3 will measure the voltage and current from the grid to guarantee operation with power factor equal to one, and finally Sensor 2 will measure the DC-link voltage at the input side of the DC-AC converter. The measurement of this voltage is important for safety and to avoid overvoltage in the circuit.

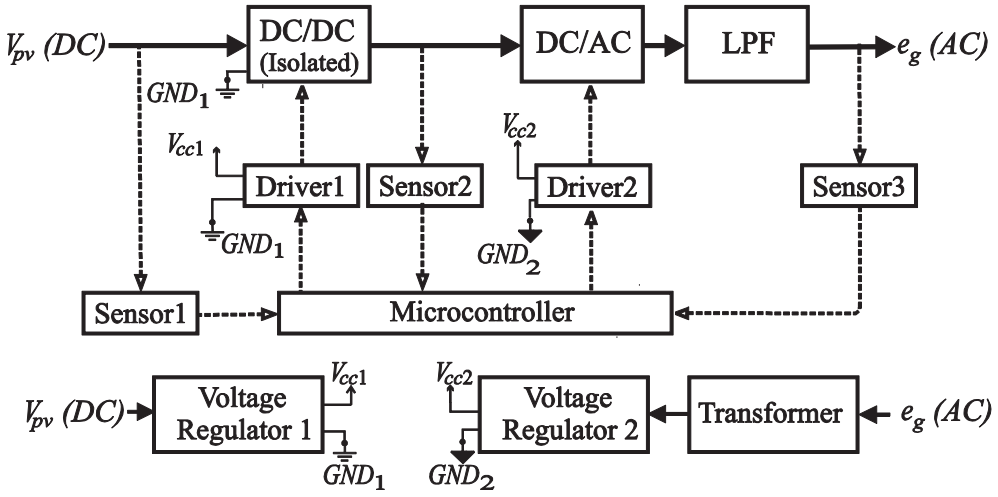

Fig. 3. Block diagram of the proposed microinverter.

III. DC-AC CONVERTER

A. Model

The proposed DC-AC converter is composed of four switching power devices (S_{1a}, S_{2a}, S_{1b}, and S_{2b}), two diodes (D_1 and D_2) and one split-wound coupled inductor. The state of the switches can be represented by a binary variable, where $S_j = 0$ means open switch and $S_j = 1$ means closed switch (with $j = 1a, 2a, 1b$, and $2b$). It is assumed that the currents in the coupled-windings are in continuous conduction mode.

The voltages v_{1a0} and v_{2a0} (voltages from the cathode of diode D_1 to zero and from the anode of diode D_2 to zero, respectively) can be expressed as a function of the state of the switches, as below:

$$v_{1a0} = S_{1a} V_{dc} \tag{1}$$

$$v_{2a0} = (1 - S_{2a}) V_{dc} \tag{2}$$

It means that the converter can be modeled as in Fig. 4(a). In this figure v_{b0} is the voltage from point b to zero and it is given by

$$v_{b0} = S_{1b} V_{dc} \tag{3}$$

The voltages v_{a0} will be given by

$$v_{a0} = (v_{1a0} + v_{2a0})/2 \tag{4}$$

Once the voltages v_{a0} and v_{b0} were obtained, then the load voltage is given by

$$v_l = v_{a0} - v_{b0} \tag{5}$$

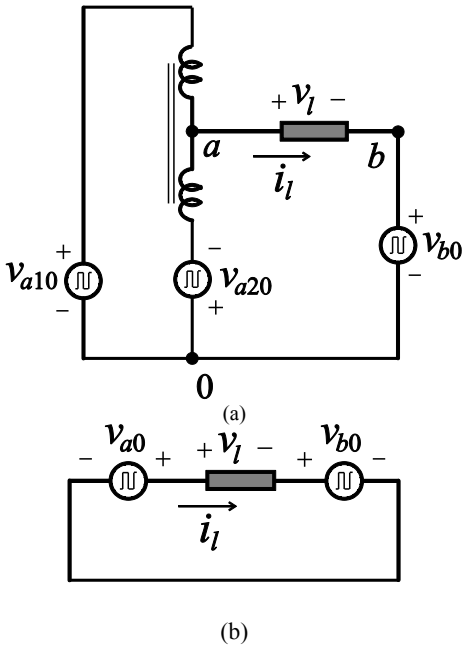

Fig. 4. (a) Converter model and (b) the simplified converter model of the proposed microinverter design.

From (5) it is possible to simplify and model the converter as depicted in Fig. 4(b).

B. PWM strategy

The gating signals S_{1a}, S_{1b}, S_{2a}, and S_{2b} must be defined to obtain a reference output voltage (v_l^*). The equation for the PWM is presented below:

$$v_l^* = S_{1a} \frac{V_{dc}}{2} + (1 - S_{2a}) \frac{V_{dc}}{2} - S_{1b} V_{dc} \tag{5}$$

Equation (5) is expressed as an instantaneous expression. The duty cycle of each switch can then be defined as:

$$D_i = \int_t^{t+T_s} S_i(t) dt \tag{6}$$

Where i = $1a$, $2a$, $1b$, or $2b$. Then, in terms of average values, equation (5) can be written as:

$$\frac{2v_l^*}{V_{dc}} = D_{1a} + 1 - D_{2a} - 2D_{1b} \tag{7}$$

With one solution for D_{1a} and D_{2a} would be:

$$D_{1a} = \frac{2v_l^*}{2V_{dc}} + S_{1b} \text{ and } D_{2a} = \frac{-2v_l^*}{2V_{dc}} + 1 - S_{1b} \tag{8}$$

After the voltage v_l^* is obtained, the signal S_{1b} must be defined with the following rules for operation: $S_{1b} = 1$ if $v_l^* < 0$ and $S_{1b} = 0$ if $v_l^* > 0$. It should be noted that leg b is operating with the same frequency as the load, which advantageously reduces switching losses. Gate signals derived from the previous equations are visualized in Fig. 5.

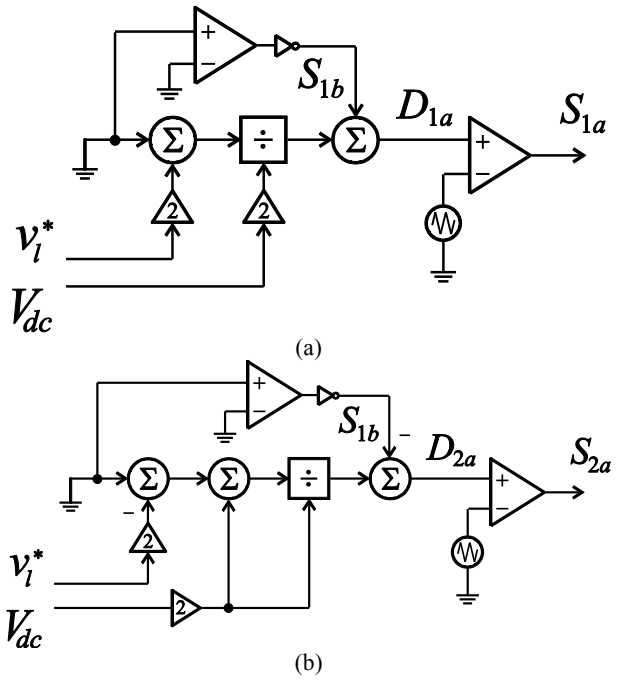

Fig. 5. Analog PWM control strategies of (a) leg 1a and (b) leg 2a.

III. DC-DC CONVERTER

Microinverters use a boost converter to step up the dc voltage from the solar panel, typically from 18-35V_{dc}, to the desired rms voltage of the system, typically grid voltage. For the proposed design, a flyback topology is used to implement the DC-DC converter. As seen in figure 2, the use of the transformer is to obtain the boosted voltage (depending on the ratio of the windings), and to achieve isolation between the solar panel voltage and the grid voltage. Since this is a conventional solution, details regarding the modes of operation for the DC-DC converter will not be presented in this digest.

IV. CONVERTER LOSSES COMPARISON

The power conversion losses have been analyzed considering both types of semiconductor losses, i.e., conduction and switching losses. Also the losses from the controlled power switches have been computed separately from the diode losses.

A comparison of the proposed configuration with the conventional one (see Fig. 6) was considered to highlight the benefits of the design of the proposed microinverter. Notice that the difference between the microinverter presented in Fig. 6 with the proposed one is on the DC-AC conversion unit.

Figs. 7(a), 7(b), and 7(c) show the switching losses (D_{sw}), conduction losses (D_{cond}) and total losses (D_{total}=D_{sw} + D_{cond}) of all diodes. The outcomes presented in Fig. 7 show that the switching losses on the diodes are predominant in a microinverter circuit. This is expected due to the low power range that this type of device operates, which in this analysis ranges from 100 W to 400 W. Furthermore, the proposed microinverter presents lower losses for all range of switching frequency and input power. It is worth mentioning that since the proposed microinverter presents an output voltage with higher quality, the switching frequency of the proposed converter was reduced to match the THD of the output waveform generated by both converters, i.e., conventional and proposed. For instance, the operation at 20 kHz of the conventional converter was compared with the proposed one operating at 7.5 kHz. This means that both converters were generating waveforms with the same quality (THD) and therefore a fair comparison was established.

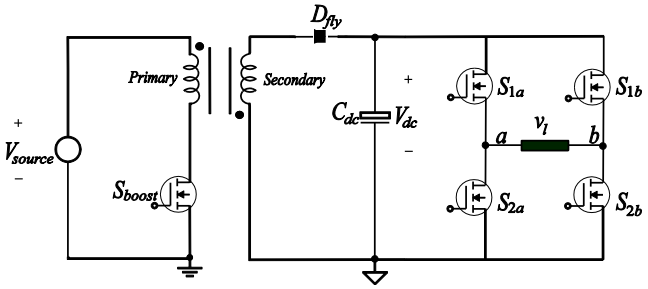

Fig. 6. Power components of a conventional microinverter.

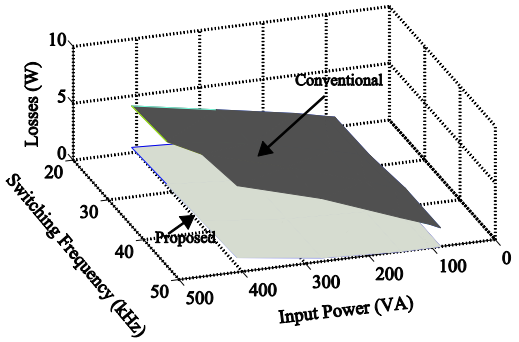

(a)

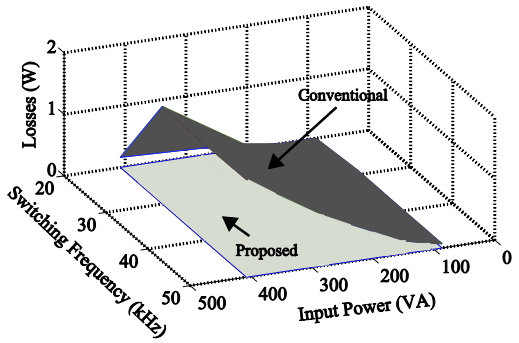

(b)

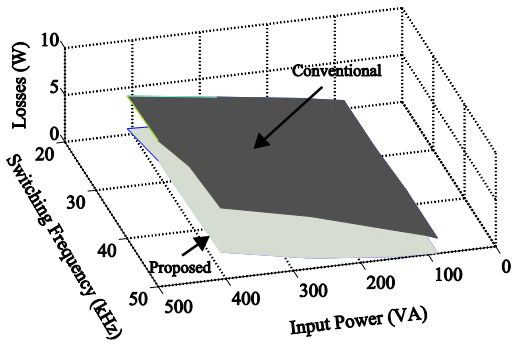

(c)

Fig. 7. Diode losses: (a) switching losses, (b) conduction losses and (c) total losses.

Fig. 8 shows a similar set of results as presented in Fig. 7 but with losses on the switch devices. Figs. 8(a), 8(b), and 8(c) show the switching losses (S_{sw}), conduction losses (S_{cond}) and total losses ($S_{total} = S_{sw} + S_{cond}$) of all controlled switches. Notice that the conduction losses of the switches are very sensitive to the amount of power processed the microinverter. Therefore, the difference in losses between the topologies is negligible.

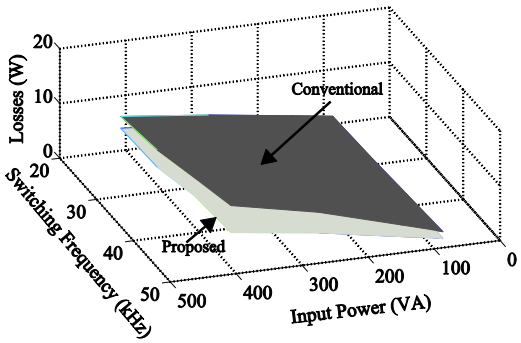

(a)

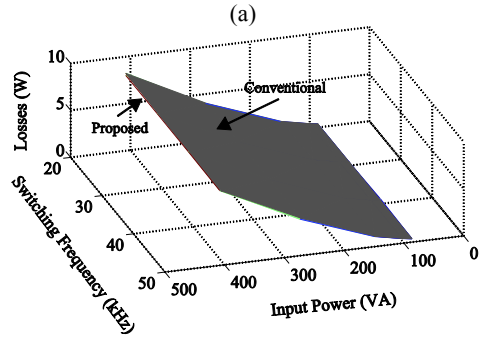

(b)

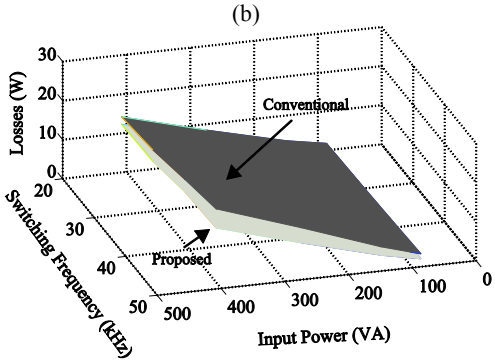

(c)

Fig. 8. Switch losses: (a) switching losses, (b) conduction losses, and (c) total losses.

Fig. 9 shows the total losses of both proposed and conventional converters including losses of the diodes and power switches. As expected from the previous analysis, the proposed design has a reduction of losses when compared with a conventional design.

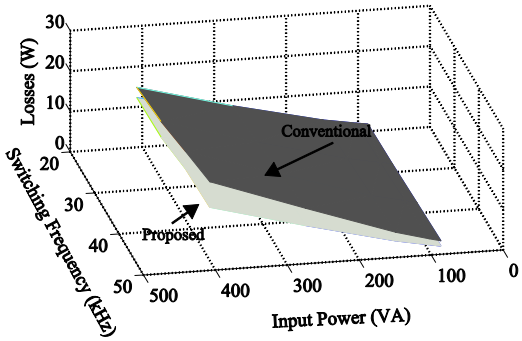

Fig. 9. Comparison of total losses between designs.

V. Experimental Results

The microinverter circuit was simulated by using PSIM® with a closed loop control strategy, while the experimental results were collected with the laboratory prototype presented in Fig. 10. Fig. 11 shows the input voltage and the DC-link voltage for the flyback topology. It also shows the simulation and experimental output voltage of the DC-AC converter v_l and the switch voltage v_{S1b}.

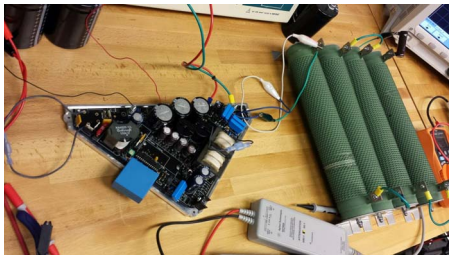

Fig. 10. Experimental setup.

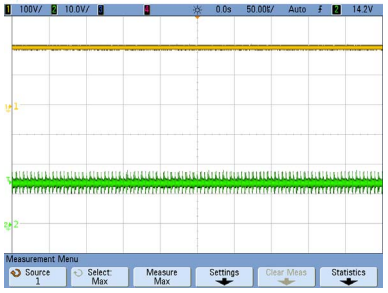

(a)

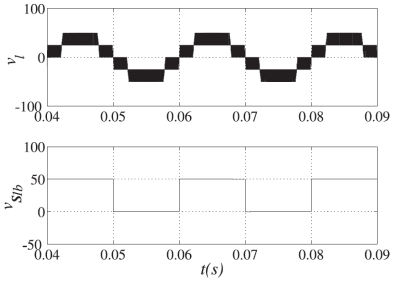

(b)

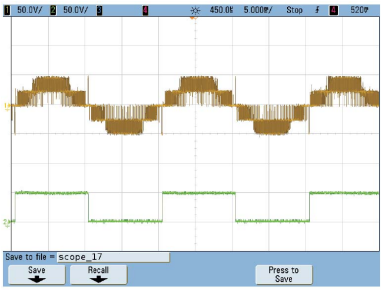

(c)

Fig. 11. (a) Input voltage (green) and dc-link voltage (yellow). (b) Simulation results of output voltage and switch voltage. (c) Experimental results of the output voltage and switch voltage.

VI. Conclusions

This paper proposes a single-phase microinverter with five levels of output PWM voltage. This increase, from the industry standard of only three levels, was obtained by using a split-wound coupled inductor in conjunction with an improved PWM strategy driving four switches. The proposed topology's most important characteristics are: (i) a reduced number of semiconductor devices, while keeping an increased number of levels at the output, (ii) a sole DC source without the need to balance capacitor voltages, and (iii) reduced semiconductor losses. These three advancements compose the highly efficient microinverter for use in industrial, commercial, and residential photovoltaic systems.

Acknowledgement

The authors of this work would like to acknowledge the Purdue School of Engineering and Technology's Electrical and Computer Engineering Department and Chair, Dr. Brian King.

References

[1] C. A. Christodoulou, N. P. Papanikolaou and I. F. Gonos, "Design of Three-Phase Autonomous PV Residential Systems With Improved Power Quality," in IEEE Transactions on Sustainable Energy, vol. 5, no. 4, pp. 1027-1035, Oct. 2014.

[2] H. Ghoddami and A. Yazdani, "A Single-Stage Three-Phase Photovoltaic System With Enhanced Maximum Power Point Tracking Capability and Increased Power Rating," in IEEE Transactions on Power Delivery, vol. 26, no. 2, pp. 1017-1029, April 2011.

[3] H. Hu, S. Harb, N. H. Kutkut, Z. J. Shen and I. Batarseh, "A Single-Stage Microinverter Without Using Eletrolytic Capacitors," in IEEE Transactions on Power Electronics, vol. 28, no. 6, pp. 2677-2687, June 2013.

[4] M. Chen, K. K. Afridi and D. J. Perreault, "A Multilevel Energy Buffer and Voltage Modulator for Grid-Interfaced Microinverters," in IEEE Transactions on Power Electronics, vol. 30, no. 3, pp. 1203-1219, March 2015.

[5] A. Nabae, I. Takahashi, and H. Akagi, "A new neutral-point clamped pwm inverter," Industry Applications. IEEE Transac- tions on, vol. lA- l 7 , pp. 5 1 8 -523 , Sept. 1981.

[6] S. Mariethoz and A. Rufer, "New configurations for the threephase asymmetrical multilevel inverter," in Industry Applications Conference. 2004. 39th lAS Annual Meeting. Conference Record of the 2004 IEEE, vol. 2, pp. 828 - 835 vol.2, Oct. 2004.

[7] H. Weng, K. Chen, J. Zhang, R. Datta, X. Huang, L. Garces, R. Wagoner, A. Ritter, and P. Rotondo, "A four-level converter with optimized switching patterns for high-speed electric drives," in Power Electronics Specialists Conference, 2007. PESC 2007. IEEE, pp. 1 5 8 5 - 1 59 1 , June 2007 .

[8] S . Kouro, M . Malinowski, K. Gopakumar, J. Pou, L. Franquelo, B. Wu, J. Rodriguez, M. Pe andrez, and J. Leon, "Recent advances and industrial applications of multilevel converters," Industrial Electronics, IEEE Transactions on, vol. 57, pp. 2553 -2580, Aug. 2010.

[9] P. Chan, H.-H. Chung, and S. Hui, "A generalized theory of boundary control for a single-phase multilevel inverter using second-order switching surface," Power Electronics, IEEE Transactions on, vol. 24, pp. 2298 -23 1 3 , Oct. 2009.

[10] A. B oora, A. Nami, F. Zare, A. Ghosh, and F. Blaabjerg, "Voltage-sharing converter to supply single-phase asymmetrical four-level diode-clamped inverter with high power factor loads," Power Electronics, IEEE Transactions on, vol. 25, pp. 2507 - 520, Oct. 20 1 0 .

[11] E. Villanueva, P. Correa, J. Rodriguez, and M. Pacas, "Control of a single-phase cascaded h-bridge multilevel inverter for gridconnected photovoltaic systems," Industrial Electronics, IEEE Transactions on, vol. 56, pp. 4399 -4406, Nov. 2009.

[12] S. Daher, J. Schmid, and F. Antunes, "Multilevel inverter topologies for stand-alone pv systems," Industrial Electronics, IEEE Transactions on, vol. 55, pp. 2703 -27 1 2 , july 2008.

[13] R. Gonzalez, E. Gubia, J. Lopez, and L. Marroyo, "Transformerless single-phase multilevel-based photovoltaic inverter," Industrial Electronics, IEEE Transactions on, vol. 5 5 , pp. 2694-2702, July 2008.

[14] E. B abaei, "A cascade multilevel converter topology with reduced number of switches," Power Electronics, IEEE Transactions on, vol. 23 , pp. 2657 -2664, Nov. 2008.

[15] B . Lin and C. Huang, "Single-phase switching-mode rectifier with capacitor-clamped topology," Electric Power Applications, lEE Proceedings - , vol. 1 52, pp. 9 - 1 6 , Jan. 2005.

[16] H. Radermacher, B . Schmidt, and R. De Doncker, "Determination and comparison of losses of single phase multi-level inverters with symmetric supply," in Power Electronics Specialists Conference, 2004. PESC 04. 2004 IEEE 35th Annual, vol. 6, pp. 4428 - 443 3 Vo1.6, June 2004.

[17] R. Li, N. Froleke, and J. Bocker, "Analysis and design of a novel three-level IIcc inverter supplying an airborne piezoelectric brake actuator," in Power Electronics Specialists Conference, 2007. PESC 2007. 1EEE, pp. 2 1 55 -2 1 6 1 , June 2007.

[18] S. Rahmani and K. AI-Haddad, "A single phase multilevel hybrid power filter for electrified railway applications," in Industrial Electronics, 2006 IEEE International Symposium on, vol. 2, pp. 925 -930, July 2006.

[19] A. Chen, C. Zhang, H. Ma, and Y. Deng, "A novel multilevel inverter topology with no clamping diodes and flying capacitors," in Industrial Electronics, 2008. IECON 2008. 34th Annual Conference of IEEE, pp. 3 1 84 -3 1 87 , Nov. 2008.

[20] S . Pulikanti and V. Agelidis, "Five-level active npc converter topology : She-pwm control and operation principles," in Power Engineering Conference, 2007. AUPEC 2007. Australasian Universities, pp. 1-5 , dec. 2007.

[21] R. Guedouani, B . Fiala, E. M. Berkouk, and M. S. Boucherit, "Control of capacitor voltage of three phase five-level npc voltage source inverter. application to inductor motor drive. ," in Electrical Machines and Power Electronics, 2007. ACEMP '07. International Aegean Conference on, pp. 794 -799, sept. 2007.

[22] Z. Li, P. Wang, Y. Li, and F. Gao, "A new single-phase five-level inverter with no problem of voltage balancing," in Energy Conversion Congress and Exposition (ECCE), 2011 IEEE, pp. 2065 -2071 , sept. 2011.

[23] R . Silva, L . Barreto, D . Oliveira, G . Henn, P. Praca, M . Heldwein, and S. Mussa, "Five-level hybrid converter based on a half-bridge/anpc cell," in Power Electronics Conference (COBEP), 201 1 Brazilian, pp. 898 -902, sept. 2011.